HHS Public Access

Author manuscript

Thromb Res. Author manuscript; available in PMC 2016 June 01.

Published in final edited form as:

Thromb Res. 2016 April ; 140(Suppl 1): S27–S36. doi:10.1016/S0049-3848(16)30095-0.

Activated tumor cell integrin αvβ3 cooperates with platelets to promote extravasation and metastasis from the blood stream

Martin R. Weber[1,*], **Masahiko Zuka**[1,*], **Mihaela Lorger**[1], **Mario Tschan**[1], **Bruce E. Torbett**[1], **Andries Zijlstra**[3], **James P. Quigley**[3], **Karin Staflin**[1], **Brian P. Eliceiri**[4], **Joseph S. Krueger**[1], **Patricia Marchese**[1], **Zaverio M. Ruggeri**[1], and **Brunhilde H. Felding**[1,2]

[1]Department of Molecular and Experimental Medicine, The Scripps Research Institute, La Jolla, California

[2]Department of Chemical Physiology, The Scripps Research Institute, La Jolla, California

[3]Department of Cell Biology, The Scripps Research Institute, La Jolla, California

[4]Department of Surgery, University of California San Diego, San Diego, CA 92103

Abstract

Metastasis is the main cause of death in cancer patients, and understanding mechanisms that control tumor cell dissemination may lead to improved therapy. Tumor cell adhesion receptors contribute to cancer spreading. We noted earlier that tumor cells can expressing the adhesion receptor integrin αvβ3 in distinct states of activation, and found that cells which metastasize from the blood stream express it in a constitutively high affinity form. Here, we analyzed steps of the metastatic cascade *in vivo* and asked, when and how the affinity state of integrin αvβ3 confers a critical advantage to cancer spreading. Following tumor cells by real time PCR, non-invasive bioluminescence imaging, intravital microscopy and histology allowed us to identify tumor cell extravasation from the blood stream as a rate-limiting step supported by high affinity αvβ3. Successful transendothelial migration depended on cooperation between tumor cells and platelets involving the high affinity tumor cell integrin and release of platelet granules. Thus, this study identifies the high affinity conformer of integrin αvβ3 and its interaction with platelets as critical for early steps during hematogenous metastasis and target for prevention of metastatic disease.

Keywords

Integrin activation; metastasis; blood stream; platelets; extravasation

Introduction

As cancer progresses, tumor cells disseminate from primary tumors to distant sites via the lymphatics or blood stream. Circulating tumor cells attach to the microvasculature of target organs, penetrate the vessel wall, and survive and proliferate within their new tissue

Correspondence to B Felding, Department of Chemical Physiology, MEM 150, The Scripps Research Institute, 10550 North Torrey Pines Road, La Jolla, CA 92037, ; Email: brunie@scripps.edu

*MR Weber and M Zuka contributed equally to this work

microenvironments. Each step can be rate limiting and involve adhesion receptors such as integrins ([1]). Integrins are heterodimeric transmembrane receptors that recognize extracellular matrix proteins and may exist in high or low affinity states. The affinity can determine ligand recognition and signals that impact cell survival, adhesion, migration, and invasion ([2–7]). Integrin affinity is regulated inside the cell and controls the adhesive phenotype and ability to bind soluble ligand ([8]). Integrin activation to high affinity is especially important for leukocytes and platelets, which circulate within the blood stream and can abruptly change their adhesive properties upon stimulation to interact with the vessel wall at sites of inflammation or vascular injury ([9–11]). Integrin activation can further control cell mobilization from bone marrow and other tissues to enter the circulation and relocate to distant tissue niches ([12]).

We previously showed that human tumor cells can express the adhesion receptor integrin αvβ3 in distinct states of activation and that tumor cells carrying the high affinity form of the receptor metastasize most efficiently ([13]). Here, we asked which steps of the metastatic cascade are influenced by integrin activation in tumor cells, and which mechanisms are involved in integrin activation-dependent metastasis. Having evidence *in vitro* that high affinity αvβ3 enables tumor cells to interact with platelets during blood flow and arrest at components of the vessel wall ([13,14]), support activation of metalloproteinase MMP-9 and invasive tumor cell migration ([15]), we now followed steps of the metastatic cascade *in vivo*. We used chick embryos and immune deficient mice to examine if, when, and how expression of activated αvβ3 confers a critical advantage to disseminating tumor cells. Following metastasis by real time PCR, non-invasive bioluminescence imaging, intravital microscopy, and histology, we analyzed the impact of αvβ3-activation on primary tumor growth, intravasation, tumor cell dissemination, and target organ colonization. The results indicate that expression of high affinity tumor cell αvβ3 is not required for primary tumor growth, but does promote initial steps of target organ colonization from the blood stream to multiple metastatic sites. The mechanism by which activated αvβ3 supports tumor cell access to target tissues depends on platelets which assist tumor cell extravasation.

Materials and Methods

Cell lines, labeling, and *in vivo* model

MDA-MB 435 human tumor cells were from Dr. Janet Price (MD Anderson). Variants of the parental cells lacking αvβ3 and reconstituted with αvβ3WT or αvβ3D723R were previously described ([13]). Clone E9 cells were isolated by limiting dilution of the parental cells. Parent Combo cells represent a pool of 20 clones, each expressing non-activated αvβ3 based on *in vitro* migration and blood perfusion as detailed below. BCM2 were isolated from MDA-MB 435 parental cells, after adding these to human blood, perfusing them across immobilized collagen I at a venous wall shear rate, and recovering the adherent tumor cells. M21 human melanoma cells express activated αvβ3 as reported ([16]). For *in vivo* tracking, the tumor cells were stably transduced with red fluorescent protein (*dsRed2*) or firefly luciferase (*F-luc*) using a self-inactivating lentiviral vector ([17]). For hematogenous metastasis, 1×10^5 or 1×10^6 tumor cells were injected into the tail vein of 5- to 8-week old female C.B17/lcTac-*Prkdc scid* mice (Taconic) and metastatic activity followed by non-invasive bioluminescence

imaging (IVIS200) ([18]), fluorescence microscopy of lung whole mounts, or by real time PCR of human *alu* sequences in lung extracts using sense primer 5' ACG CCT GTA ATC CCA GCA CTT 3' and antisense primer 5' TCG CCC AGG CTG GAG TGC A 3' ([19]).

Induction of thrombocytopenia and in vivo tumor cell extravasation

Thrombocytopenia was induced by i.v. injecting SCID mice with anti-murine GPIbα (CD42b) (Emfret) (3 μg/g bodyweight). Platelet counts were measured using an automated blood cell counter adjusted to murine blood. Tumor cells were injected 4 h after induction of thrombocytopenia. Tumor cell extravasation from the pulmonary microvasculature was analyzed 3 days later. The lungs were inflated with 10% neutral buffered formalin through the trachea, post fixed, and cryosectioned (35μm sections). The endothelium was stained with anti-CD31 (PECAM) and tumor cells with anti-human CD44. Quantification was performed using a Zeiss Axio Imager M1m microscope, which allowed for analysis of a large number of events. Localization of cancer cells inside or outside the vasculature was confirmed by confocal microscopy with a 40× water immersion objective using an Olympus IX81 equipped with UltraVIEW VoX Confocal Imaging System (Perkin Elmer). Images were acquired and analyzed with Velocity software.

Flow cytometry

Integrin expression and αvβ3 activation state were analyzed by flow cytometry (FACS Calibur, Becton Dickinson) with anti αvβ3 mAb VNR1-27.1 ([20]), or activation-dependent human ligand-mimetic scFv antibodies Bc-12 and Bc-15 ([16]). ScFv binding was detected with M2 mouse anti-FLAG and anti-mouse-APC using TBS with or without 1mM EDTA, 1mM Ca^{2+}, or 0.1 mM Mn^{2+} as binding and washing buffer.

In vitro migration and arrest during blood flow

Haptotactic migration toward human extracellular matrix proteins was detailed earlier ([15]). Cancer cell arrest during blood flow was measured as described ([13]). Briefly, dsRed tagged tumor cells (red fluorescence) were suspended in human blood anticoagulated with 50 nM -Pro-Arg-chloro methyl ketone (PPAK), spiked with 10 μM mepacrine (green fluorescence) and perfused over collagen I or subendothelial matrix at a venous wall shear rate of 50 s^{-1} (4 dynes/cm^2). Adhesive events and cell interactions were recorded by fluorescence video microscopy and quantified at 50 predefined positions by image analysis using MetaMorph software. Tumor cell-platelet interaction during blood flow was further analyzed with a dual laser system (486 nm and 580 nm) and differentiating band pass filters (510 nm and 580 nm), using calcein-green labeled tumor cells and calcein-red labeled mouse platelets, reconstituted into platelet-poor murine plasma anticoagulated with heparin. Tumor cell-platelet interactions were recorded by digital video microscopy and analyzed with MetaMorph software.

Dorsal skin fold chamber and intravital microscopy

Tumor cell interaction with the pulmonary microvasculature was observed by intravital microscopy in lung allografts grown in dorsal skin fold chambers on SCID mice as described ([21]). Briefly, titanium frames were implanted into a dorsal skin fold, transplanted

with SCID lung allografts 3 days later, and allowed to vascularize for 14 days. The allografts were superfused with TNFα (50μl at 1μg/ml) 2.5 hours before injecting 2.5×10^6 dsRed tagged tumor cells i.v. together with FITC-dextran (500 kDa) to visualize the vasculature. Adhesive events were observed with an intravital microscope (Leitz Biomed) ([21]).

Transendothelial migration and platelet preparation

Human pulmonary microvascular endothelial cells were grown for 5 days on transwell filters (8 μm pores) coated with human fibronectin (10μg/ml). Monolayer integrity was measured by transendothelial resistance. Conditioned medium from IMR-90 fibroblasts in the lower chamber was used to attract tumor cells (4×10^4) seeded atop the endothelial layer during a 16 hr migration period. Where indicated, washed human platelets (433×10^3/μl) were added to the tumor cell suspension, with or without stimulation with thrombin receptor activating peptide TRAP-6 (12.5 μM). Non-migrated tumor cells were removed from the filter tops with cotton swaps, filters fixed in 4% paraformaldehyde, and transmigrated tumor cells counted by fluorescence microscopy on the filter underside in 5 optical fields. Effects of platelets and their releasates on the integrity of human pulmonary endothelial monolayers in the presence of tumor cells was measured by incubating intact endothelial layers (transendothelial resistance >30Ω/cm^2) with BCM2 cells and washed human platelets stimulated with ADP, or with platelet releasates for increasing time periods at 37 °C and 5% CO_2.

Results

Heterogeneous tumor cells contain a subset that expresses activated integrin αvβ3

To identify critical steps within the metastatic cascade affected by the activation state of integrin αvβ3 and to analyze mechanisms involved, we generated a model of tumor cell of variants with a common genetic background and defined levels of αvβ3 expression and activation. We chose MDA-MB 435 human breast cancer cells because of their aggressive metastatic behavior in immune deficient mice, which makes them suitable for following individual steps of the metastatic cascade ([22–24]). The majority of MDA-MB 435 parental cells express integrin αvβ3. Here we show that subpopulations exist within the parental cells, which express αvβ3 in a constitutively high affinity form and that these cells have a functional advantage during metastatic dissemination. To isolate cells with defined states of αvβ3 activation without *in vivo* selection, which may favor additional properties unrelated to αvβ3, we cloned MDA-MB 435 cells by limiting dilution and analyzed 25 individual clones for αvβ3 expression and activation state. Clone E9 was identified as carrying αvβ3 in a constitutively activated form because it bound soluble αvβ3 ligands, including the αvβ3 specific ligand-mimetic scFv antibody Bc-15. This scFv contains an RGD integrin-binding motif typical for αvβ3 ligands within CDR-H3 ([16]). Twenty cell clones, each of which expressed αvβ3 but failed to bind Bc-15 and other soluble αvβ3 ligands were pooled and named Parent Combo. These cells uniformly express non-activated αvβ3. Furthermore, a polyclonal variant termed BCM2 was isolated after perfusing MDA-MB 435 parental cells, mixed into human blood, across a thrombogenic collagen I matrix at a venous wall shear rate. The arrest competent cells, BCM2, were expanded and reanalyzed in blood perfusion studies, revealing that the cells uniformly express high affinity αvβ3. For comparison, we

used MDA-MB 435 cell variants that we previously generated to express defined states of αvβ3 activation. β3D723R cells were generated by reconstituting a β3-lacking subpopulation of MDA-MB 435 ($\beta3^{minus}$) with the activating β3 mutant gene. Reconstitution with the β3 wild type gene (β3WT) results in non-activated αvβ3 expression ([13]). αvβ3 expression and activation in the cell variants used in this study are summarized in supplemental Fig. S1.

Before investigating steps of the metastatic cascade where the activated form of tumor cell integrin αvβ3 exerts its pro-metastatic properties, we verified the functional activation state of the receptor in our cell model. Cells carrying the activating mutant β3D723R were compared against $\beta3^{minus}$ cells, activated clone E9, and non-activated pool Parent Combo. We analyzed two metastasis related tumor cell functions that are mediated by integrin αvβ3 and which require the activated, high affinity state of the receptor ([25];[26]). One functions is migration toward a fibrinogen substrate, which is exclusively supported by αvβ3 on these cells ([15]). The other function is tumor cell attachment to components of the vessel wall during blood flow. This process depends on activated αvβ3 binding of soluble plasma proteins, such as fibrinogen, which cross-links the tumor cells with platelets and then supports the arrest event ([14]). We found that clone E9 and the β3D723R expressing cells, but not the $\beta3^{minus}$ and Parent Combo cells, migrated actively toward fibrinogen. This was blocked by an inhibitory anti-β3 antibody (Fig. 1A). Consistent with this finding, clone E9 and β3D723R expressing cells, but not $\beta3^{minus}$ and Parent Combo cells, were able to arrest on a collagen I matrix during blood flow in a platelet-dependent manner. The interaction of clone E9 and β3D723R cells with platelets during blood flow, and the ability of the tumor cells to arrest were inhibited by a function blocking anti-αvβ3 antibody (Fig. 1B). BCM2 cells behaved like clone E9 and β3D723R cells, confirming αvβ3 activation (not shown). Cells expressing β3WT that failed to bind soluble ligand also failed to interact with platelets and arrest during blood flow, confirming that αvβ3 is not activated (Fig. 1B). Thus, subpopulations of tumor cells expressing constitutively activated integrin αvβ3 can exist within a heterogeneous cell population which at large carries the non-activated receptor. During blood flow, cells with high affinity αvβ3 are selected based on the ability of the receptor to support cell arrest.

As an additional tumor cell model, we included M21 human melanoma cells. We showed earlier that these cells express high affinity αvβ3 and use the receptor for interaction with platelets and cell arrest in flowing blood ([14];[25]). The dynamics of the interaction during the arrest process is documented here in the video attached to Fig. 1C. It reveals that blood borne tumor cells can anchor on platelets and utilize platelets for cohesion. A dual-laser analysis of calcein-green tagged M21 cells, perfused in blood reconstituted with calcein-red tagged platelets, showed that tumor cells interacting with platelets can rapidly extend pseudopods (Fig. 1D). This likely supports the anchoring process seen in the video. M21-L cells, an αv integrin lacking variant of M21, cannot engage in this interaction and fails to arrest ([14]).

Activation of tumor cell integrin αvβ3 promotes initial steps of target organ colonization from the blood stream, but does not affect primary tumor growth

To identify steps within the metastatic cascade in which the activation state of tumor cell integrin αvβ3 limits success, we first examined the ability of the cells to form a primary tumor. This was done in chick embryos and in the mammary fat pad of SCID mice. The chick model was chosen because it also allows for analysis of tumor cell dissociation from a primary tumor and intravasation ([19]). After inoculating tumor cells (2×10^6) expressing activated mutant receptor αvβ3D723R versus cells expressing non-activated αvβ3WT onto the chorioallantoic membrane (CAM) near the allantoic vein of 10 day old chick embryos, tumors were induced by each cell line and grew at similar rates. They also showed similar rates of intravasation, measured by the number of tumor cells in the lower CAM seven days after implantation (578±346 β3D723R, 641±225 β3WT, n=7/group). Quantification was based on real time PCR of the human *alu* sequences, as described ([19]). Interestingly, in the mammary fat pad of SCID mice, representing the primary tumor site, $\beta3^{minus}$ cells grew more rapidly than β3WT and β3D723R expressing cells (Fig. 2A). However, $\beta3^{minus}$ tumors did not metastasize and spontaneous lung lesions came primarily from tumors expressing activated β3D723R. Occasional lung lesions were also found in mice with β3WT tumors. FACS analysis of tumor cells from those lung lesions for soluble ligand binding (ligand mimetic antibody) revealed that αvβ3 was expressed in the high affinity form by the cells that had metastasized (not shown). This indicates that activated αvβ3 fosters metastasis. Together, expression of αvβ3 and its functional activation state apparently do not limit tumor formation at a primary site or the ability of tumor cells to gain access to the circulation, but do play a critical role during the subsequent steps of metastasis.

We next examined tumor cell colonization of target organs from the blood stream. At this stage, activated αvβ3 provided the tumor cells with a clear advantage. Following tumor cell arrest and expansion in the lungs of SCID mice by fluorescence microscopy and *alu* PCR, indicated that cells expressing activated αvβ3D723R remained in the pulmonary vascular bed and developed metastatic foci more successfully than cells carrying non-activated αvβ3WT (Fig. 2B,C). Of 1×10^6 injected cells, $8.5–9.5\times10^5$ were found in the lungs 3 hours later regardless of αvβ3 activation. For both cell types, this number dropped sharply within the next 12 hours and reached a low point at 24 hours. At this time and during the following 18 days, β3WTexpressing cells were barely detectable in the lungs while β3D723R carrying cells maintained a level of about 1×10^5 cells at 24 hours and then increased steadily, exceeding 2.5×10^8 cells compared to only 8×10^5 β3WT cells on day 35 (Fig. 2B). Clearance of tumor cells from lung tissue within the first 24 hours and the early advantage of the β3D723R expressing cells were confirmed by fluorescence microscopy, monitoring dsRed tagged cells within the lungs (Fig. 2C). Intravital microscopy of lung tissue grafts, grown within dorsal skin fold chambers on SCID mice, allowed to detect the arrest process of β3D723R expressing cells within the pulmonary microvasculature (Fig. 2D). While the arrest events were rare and not suitable for quantification, as only small tissue areas could be observed over time, the captured images provide evidence that activated αvβ3 expressing cells can successfully arrest within the pulmonary vascular bed. No arrest events were observed after injection of non-activated β3WT expressing cells. Together, these results indicate that high-affinity integrin αvβ3 endows circulating tumor cells with functional

properties that enhance their ability to colonize the lungs from the blood stream. This initial advantage of tumor cells carrying high affinity αvβ3 translates into enhanced metastatic burden over time.

Integrin αvβ3 activation promotes hematogenous metastasis to multiple sites

We next asked if the advantage conferred to tumor cells by the high affinity receptor is specific for colonizing the lung, or if αvβ3 activation more generally promotes metastasis from the blood stream. To address this question, we compared firefly luciferase (F-*luc*) tagged variants of our cell model that carry intrinsically activated versus non-activated αvβ3 by non-invasive bioluminescence imaging for development and distribution of metastatic lesions.

E9 cells, cloned *in vitro* from the parent, express intrinsically activated αvβ3 (Fig. 1). When injected into the venous circulation, E9 cells actively produced metastatic lesions in the lungs and other target organs. In contrast, Parent Combo cells, representing a pool of 20 clones with non-activated αvβ3, poorly colonized the lungs and other sites. Figure 3A shows typical organ distribution and quantification of metastatic burden in the lungs comparing clone E9 and Parent Combo cells. The differences in lung colonization were statistically significant when measured 14 days after tail vein injection of 1×10^5 tumor cells, as well as 34 days after injecting 1×10^6 tumor cells to challenge the system. *Ex vivo* imaging of excised target organs on day 56 revealed increased incidence of metastasis to multiple sites for clone E9 expressing the activated integrin (Fig. 3B). This enhancement of overall metastatic activity and potential to colonize most major target organs of metastasis from the blood stream, was confirmed with BCM2 cells which also expresses intrinsically activated αvβ3 (Fig. 3B). Similar results were obtained with β3D723R cells carrying the experimentally activated mutant receptor. These results indicate that expression of high affinity integrin αvβ3 provides blood borne tumor cells with a critical advantage during the colonization of major target organs of metastasis.

Activated integrin αvβ3 promotes tumor cell transendothelial migration in a platelet dependent manner

To analyze mechanisms by which high affinity tumor cell integrin αvβ3 supports early steps of metastasis from the blood stream, we followed a key function of the activated integrin that initially led us to appreciate distinct affinity states of αvβ in tumor cells. This function is to promote tumor cell interaction with platelets ([13];[14]). Here, we asked if an interaction between tumor cells and platelets could promote not only initial tumor cell arrest within the target organ microvasculature, but also subsequent steps of organ colonization. After attaching to the microvascular endothelium of target organs, metastatic tumor cells penetrate the endothelial barrier before invading target tissues. To investigate this step, we analyzed the effect of αvβ3 activation on tumor cell transendothelial migration in the presence or absence of platelets (Fig. 4). Comparing cells expressing experimentally (β3D723R) or intrinsically (BCM2) activated αvβ3 against cells carrying the non-activated integrin (β3WT) revealed, that either cell type poorly penetrated monolayers of human pulmonary microvascular endothelial cells in the absence of platelets. However, when platelets were present, tumor cells with activated αvβ3 transmigrated very efficiently in contrast to cells

with the non-activated integrin. This response was not further enhanced when platelets were stimulated with thrombin receptor activating peptide (TRAP-6). Platelets that had previously released their α-granule contents failed to support tumor cell-transendothelial migration (Fig. 4A). Platelet releasate alone potentiated tumor cell-induced endothelial retraction and inhibited endothelial monolayer integrity. This was seen when intact human pulmonary endothelial layers (initial transendothelial resistance >30Ω/cm^2) were incubated with BCM2 cells, together with washed human platelets stimulated with ADP, or with ATP-induced platelet releasates (Fig. 4B). The results indicate that tumor cell interaction with platelets and proteins released from platelet granules strongly promote tumor cell penetration of lung microvascular endothelium. Importantly, this cooperation with platelets depended on the activated state of tumor cell integrin αvβ3, as cells expressing the non-activated wild type receptor (Fig. 4A) as well as those lacking αvβ3 (not shown) largely failed migrate through the endothelium, regardless of the presence of platelets.

Platelets promote tumor cell extravasation and metastasis from the blood stream

To examine if the effect of platelets on tumor cell transendothelial migration observed *in vitro* is relevant for extravasation *in vivo*, we rendered SCID mice thrombocytopenic and followed the fate of injected tumor cells within a time window of reduced platelet counts. Thrombocytopenia was induced by injecting mice with an antibody against murine platelet receptor GPIbα. This treatment reduced platelet counts 10-fold from an average of 823×10^3/μl to 72×10^3/μl four hours after antibody injection. Counts remained low for 4 days before returning to normal (Fig. 5). To examine if platelets support tumor cell extravasation within the lung microvasculature, 5×10^5 tumor cells with activated αvβ3, namely β3D723R cells, BCM2, and M21 melanoma cells were injected into the venous circulation, four hours after treatment with anti-platelet antibody when platelet counts had reached the low point. Three days later, within the time window of reduced platelet count, the lungs were examined by histology in serial sections throughout the lung tissue. As shown in Table 1, the number of detectable micrometastases for β3D723R expressing cells and BCM2 cells was strongly reduced in thrombocytopenic mice. Importantly, it was possible to discern extravasated from intravascular tumor cells by analyzing the integrity of basement membranes and the endothelium of the pulmonary microvasculature. Tumor cells clearly surrounded by intact endothelium were classified as intravascular. Tumor cells detected in thrombocytopenic animals largely failed to extravasate, while almost all tumor cells detected in mice with normal platelet counts were found outside the vasculature. Intravascular localization of tumor cells in thrombocytopenic mice, and extravascular localization in mice with normal platelet counts, was confirmed by confocal microscopy as shown for M21 and BCM2 cells in Fig. 5A. Importantly, the majority of tumor cells in mice with normal platelet counts began to proliferate and incorporate BrdU on day 3 post injection, while the percentage of BrdU-positive tumor cells was 3.6–3.9 fold reduced in thrombocytopenic animals (Tab.1). Inhibition of tumor cell extravasation and proliferation by reducing platelet counts, early during target organ colonization from the blood stream, translated into reduced numbers and sizes of metastatic foci in the lungs. This was shown on day 18 after tumor cell injection (Fig. 5C). The fact that platelet counts remained low only during the first 4 days after tumor cell injection, and then returned to normal (Fig. 5B), indicates that platelets played a major role during the initial steps of target organ colonization from the blood stream. Importantly,

this had a profound long-term effect on metastatic development. Therefore, the absence of platelets, or the inability of tumor cells to cooperate with them, can limit metastatic activity. The finding that activation of tumor cell integrin αvβ3 promotes cooperation with platelets, and only then supports tumor cell extravasation from the blood stream and colonization of target organs, provides a mechanism through which the high affinity form of this integrin promotes metastasis.

Discussion

The metastatic cascade comprises discrete steps in each of which tumor cell must succeed to establish distant lesions ([27]). Knowledge about mechanisms supporting individual steps of the dissemination process can help define molecular and functional targets for therapeutic intervention and prevention of metastatic disease. This study provides insight into the role of integrin activation in human tumor metastasis. It identifies extravasation of circulating tumor cells as a step where the affinity state of tumor cell integrin αvβ3 makes a critical contribution based on cooperation with platelets.

The adhesion receptor integrin αvβ3 allows tumor cells to attach and migrate on extracellular matrix proteins ([28]). This generates signals for cell survival, proliferation, and expression of genes that support invasion, and stromal interactions ([6;29]). We noted earlier that tumor cells can express αvβ3 in distinct states of activation, and that cells from metastatic lesions carry the integrin in a constitutively high affinity form ([13]). Importantly, targeting of the activated conformer of αvβ3 on circulating tumor cells with RGD-containing ligand mimetic antibodies from cancer patients prevented metastasis from the blood stream ([16]).

We now analyzed steps within the metastatic cascade that are specifically supported by tumor cell integrin αvβ3 and to investigate mechanisms through which high-affinity αvβ3 enhances metastatic progression. We chose a cell model where αvβ3 was identified as important for metastasis, and where αvβ3 activation is essential for metastasis ([13]). We used MDA-MB 435 cells because they exemplify a heterogeneous tumor cell population with aggressive metastatic properties. The MDA-MB 435 cell line is a basal type, triple negative human breast carcinoma line ([22]) that coexpresses epithelial and melanocytic markers, seen particularly in aggressive metaplastic breast cancers ([30–32]). The resemblance of certain attributes of MDA-MB 435 breast cancer cells ([23;24]) with melanoma ([33]), indicates a shared aggressiveness to which expression of high affinity αvβ3 contributes. Here, we show that the MDA-MB 435 cell line contains clones expressing constitutively activated αvβ3, and that these are clearly more metastatic than clones carrying the non-activated receptor. Importantly, cells with activated αvβ3 excelled at colonizing all major organs of breast cancer metastasis from the blood stream. In contrast, we found that tumor growth at the primary site was not dependent on αvβ3 expression or its activation state. Indeed, a cell variant lacking β3 formed the largest tumors in the mammary fat pad, but only high affinity αvβ3 supported spontaneous metastasis. Furthermore, our results from the chick embryo model indicate that escape from a primary tumor and intravasation did not depend on αvβ3 and its affinity state. Thus, αvβ3 activation must play a role at a later step.

To investigate the juncture at which high affinity αvβ3 critically advances metastatic progression, we used variants of the MDA-MB 435 model that share a genetic background. In these variants, αvβ3 activation was either controlled experimentally by introducing a β3 mutation that renders the heterodimer constitutively active (β3D723R) ([34]), or which were selected *in vitro* from the parental cells, based on the ability to arrest during blood flow and validated for stable functional activation of the receptor. In each of these variants, the general integrin expression profile was unaltered. This includes other αv integrins. Thus, this model allowed us to followed the specific contribution of activated αvβ3 to distinct steps of the metastatic cascade. We identified tumor cell extravasation from the blood stream as a rate-limiting step that requires high affinity αvβ3. We found, *in vitro* and *in vivo*, that successful transendothelial migration depended on a cooperation between the tumor cells and platelets, and involved the release of platelet granules. Interestingly, analysis of tumor cell-platelet interaction during blood flow revealed directly that platelets support the arrest process and immediate extension of pseudpods when tumor cells are in contact with platelets. These reactions could foster invasive tumor cell migration required for extravasation. Importantly, the essential contribution of platelets to tumor cell extravasation from the pulmonary microvasculature was seen in the breast cancer cell system, as well as in a human melanoma cell model.

Platelet α granules contain a multitude of adhesive ligands, coagulation proteins, pro and anti-angiogenic factors, growth factors, chemokines, cytokines, proteases and bioactive lipid metabolites, many of which directly affect endothelial cells and the integrity of the vascular endothelium ([35]). For example, platelet released sphingosine 1-phosphate induces rapid loss of endothelial tight junction proteins ZO-1 and Claudin-18 ([36]), and lysophosphatidic acid induces vascular permeability ([37]). Metalloproteinases, and other proteases from platelet α granules, may facilitate extravastation of leukocytes and monocytes, specifically when activated by thrombin within the platelet microenvironment ([38];[39]). Furthermore, junctional adhesion molecules, such as JAM-C and adhesion receptor GPIbα expressed on platelets, can serve as binding partners for leukocyte integrin αMβ2 and support monocyte and neutrophil extravasation, as well as recruitment of cytotoxic T cells ([40]–[44]). Such mechanisms might also be involved in the ability of platelets to support angiogenesis ([45];[46]).

Our results show that platelets and their released factors can potently promote tumor cell transendothelial migration, and that platelets are required for extravasation of circulating tumor cells *in vivo*. This platelet-mediated effect depends on the expression of high affinity tumor cell integrin αvβ3. Platelets may become activated when in contact with tumor cells within the capillary bed of target organs. This can promote endothelial permeability and allow tumor cells expressing activated αvβ3 to efficiently use the receptor for penetration of the vessel wall. Extravastion and target organ invasion could be supported by activation of MMP-9 which is enhanced by high affinity tumor cell integrin αvβ3, as we previously showed ([15]). Tumor cell binding to platelets, leading to these events, is mediated by activated αvβ3 and platelet integrin αIIbβ, crosslinked by shared multivalent ligands such as fibrinogen ([13];[14]). This interaction could promote tumor cell binding to the endothelium in a variety of capillary beds, potentially with or without help from target organ specific endothelial receptors. Indeed, our data indicate that tumor cells expressing activated αvβ3

show enhanced metastatic activity in all major target organs examined, and that reduction of platelet numbers lead to a general decrease in metastatic activity from the blood stream. This involved specific adhesive interactions and was not due to unspecific blockage of microvessels by platelet-tumor cell heteroaggregates, as seen by intravital microscopy and histology.

Recent reports highlight contributions of platelets to metastatic progression. Platelet interaction with circulating tumor cells can promote their epithelial to mesenchymal transition through TGF-β ([47;48]), as well as guide formation of early metastatic niches by secretion of CXCL-5 and CXCL-7 for recruitment of granulocytes ([49]). Physically, platelet released microparticles ([50]) and possibly neutrophil extracellular traps (NETs) consisting of DNA meshworks loaded with histones and serine proteases that contribute to adhesion and aggregation ([51]), can promote vascular tumor cell platelet interaction, tumor cell proliferation and invasiveness via a multitude of platelet released factors ([35;52–55]). Specific ligands that directly bind tumor cell integrin αvβ3 or potentiate its activation state include autotaxin ([56]) and podocalyxin ([57]), respectively, and thereby stimulate cancer cell growth and adhesive functions.

In the context of mounting evidence that platelets promote metastasis, our results show that platelets play a critical role during the initial phase after tumor cells have gained access to the circulation. Thrombocytopenia, induced at that time point, strongly inhibited tumor cell extravasation and significantly reduced metastatic burden in the long run. Cooperation between tumor cells and platelets gives tumor cells expressing high affinity αvβ3 direct, and possibly indirect advantages for target organ colonization. Thus, this study identifies the high affinity form of tumor cell integrin αvβ3, and the mechanism that promotes this phenotype, as targets for preventing early steps of metastasis from the blood stream.

Supplementary Material

Refer to Web version on PubMed Central for supplementary material.

Acknowledgments

This work was supported by NIH grants R01CA170140, R01CA170737, R21CA198595 (to B Felding), CDMRP DoD grants W81XWH-13-1-0401, W81XWH-14-1-0381 (to B Felding), California Breast Cancer Research Program grant 18IB-0022 (to B Felding), donations from the Plotkin-Weiss Family Foundation, the Mildred Scheel Stiftung fuer Deutsche Krebshilfe (Fellowship to MRW), the Swedish Research Council (Fellowship to KS), and Susan G. Komen fellowship PDF0403205 to JSK. We thank Deirdre O'Sullivan for inspiring discussions and Jane Forsyth for expert technical support.

Reference List

1. Hynes RO. The emergence of integrins: a personal and historical perspective. Matrix Biol. 2004; 23:333–340. [PubMed: 15533754]
2. Arnaout MA, Goodman SL, Xiong JP. Structure and mechanics of integrin-based cell adhesion. Curr Opin Cell Biol. 2007; 19:495–507. [PubMed: 17928215]
3. Ginsberg MH, Partridge A, Shattil SJ. Integrin regulation. Curr Opin Cell Biol. 2005; 17:509–516. [PubMed: 16099636]
4. Luo BH, Carman CV, Springer TA. Structural Basis of Integrin Regulation and Signaling. Annu Rev Immunol. 2007; 25:619–647. [PubMed: 17201681]

5. Felding-Habermann B. Integrin adhesion receptors in tumor metastasis. Clin Exp Metastasis. 2003; 20:203–213. [PubMed: 12741679]
6. Stupack DG, Cheresh DA. Get a ligand, get a life: integrins, signaling and cell survival. J Cell Sci. 2002; 115:3729–3738. [PubMed: 12235283]
7. Lim ST, Mikolon D, Stupack DG, Schlaepfer DD. FERM control of FAK function: implications for cancer therapy. Cell Cycle. 2008; 7:2306–2314. [PubMed: 18677107]
8. Banno A, Ginsberg MH. Integrin activation. Biochem Soc Trans. 2008; 36:229–234. [PubMed: 18363565]
9. Zou Z, Chen H, Schmaier AA, Hynes RO, Kahn ML. Structure-function analysis reveals discrete {beta}3 integrin inside-out and outside-in signaling pathways in platelets. Blood. 2006; 109:3284–3290. [PubMed: 17170121]
10. Cantor JM, Ginsberg MH, Rose DM. Integrin-associated proteins as potential therapeutic targets. Immunol Rev. 2008; 223:236–251. 236-51. [PubMed: 18613840]
11. Makino A, Shin HY, Komai Y, Fukuda S, Coughlin M, Sugihara-Seki M, et al. Mechanotransduction in leukocyte activation: a review. Biorheology. 2007; 44:221–249. [PubMed: 18094448]
12. Chigaev A, Waller A, Amit O, Sklar LA. Galphas-coupled receptor signaling actively down-regulates alpha4beta1-integrin affinity: a possible mechanism for cell de-adhesion. BMC Immunol. 2008; 9:26. 26. [PubMed: 18534032]
13. Felding-Habermann B, O'Toole TE, Smith JW, Fransvea E, Ruggeri ZM, Ginsberg MH, et al. Integrin activation controls metastasis in human breast cancer. Proc Natl Acad Sci U S A. 2001; 98:1853–1858. [PubMed: 11172040]
14. Felding-Habermann B, Habermann R, Saldivar E, Ruggeri ZM. Role of beta3 integrins in melanoma cell adhesion to activated platelets under flow. J Biol Chem. 1996; 271:5892–5900. [PubMed: 8621462]
15. Rolli M, Fransvea E, Pilch J, Saven A, Felding-Habermann B. Activated integrin alphavbeta3 cooperates with metalloproteinase MMP-9 in regulating migration of metastatic breast cancer cells. Proc Natl Acad Sci U S A. 2003; 100:9482–9487. [PubMed: 12874388]
16. Felding-Habermann B, Lerner RA, Lillo A, Zhuang S, Weber MR, Arrues S, et al. Combinatorial antibody libraries from cancer patients yield ligand-mimetic Arg-Gly-Asp-containing immunoglobulins that inhibit breast cancer metastasis. Proc Natl Acad Sci U S A. 2004; 101:17210–17215. [PubMed: 15563590]
17. Swan CH, Buhler B, Steinberger P, Tschan MP, Barbas CF III, Torbett BE. T-cell protection and enrichment through lentiviral CCR5 intrabody gene delivery. Gene Ther. 2006; 13:1480–1492. [PubMed: 16738691]
18. Chen EI, Hewel J, Krueger JS, Weber MR, Tiraby C, Kralli A, et al. Adaptation of energy metabolism in breast cancer brain metastases. Cancer Res. 2007; 67:1472–1486. [PubMed: 17308085]
19. Zijlstra A, Mellor R, Panzarella G, Aimes RT, Hooper JD, Marchenko ND, et al. A quantitative analysis of rate-limiting steps in the metastatic cascade using human-specific real-time polymerase chain reaction. Cancer Res. 2002; 62:7083–7092. [PubMed: 12460930]
20. Lam SCT, Plow EF, D'Souza SE, Cheresh DA, Frelinger AL, Ginsberg MH. Isolation and characterization of a platelet membrane protein related to the vitronectin receptor. J Biol Chem. 1989; 264:3742–3749. [PubMed: 2465293]
21. Sikora L, Johansson AC, Rao SP, Hughes GK, Broide DH, Sriramarao P. A murine model to study leukocyte rolling and intravascular trafficking in lung microvessels. Am J Pathol. 2003; 162:2019–2028. [PubMed: 12759257]
22. Price JE, Zhang RD. Studies of human breast cancer metastasis using nude mice. Cancer Metastasis Rev. 1990; 8:285–297. [PubMed: 2182209]
23. Chambers AF. MDA-MB-435 and M14 Cell Lines: Identical but not M14 Melanoma? Cancer Res. 2009; 96:5292–5293. [PubMed: 19549886]
24. Hollestelle A, Schutte M. Comment Re: MDA-MB-435 and M14 cell lines: identical but not M14 Melanoma? Cancer Res. 2009; 69:7893. [PubMed: 19723654]

25. Pilch J, Habermann R, Felding-Habermann B. Unique ability of integrin alpha(v)beta 3 to support tumor cell arrest under dynamic flow conditions. J Biol Chem. 2002; 277:21930–21938. [PubMed: 11934894]
26. Nag S. Morphology and molecular properties of cellular components of normal cerebral vessels. Methods Mol Med. 2003; 89:3–36. [PubMed: 12958410]
27. Langley RR, Fidler IJ. Tumor cell-organ microenvironment interactions in the pathogenesis of cancer metastasis. Endocr Rev. 2007; 28:297–321. [PubMed: 17409287]
28. Felding-Habermann B, Cheresh DA. Vitronectin its receptors. [Review] [51 refs]. Curr Opin Cell Biol. 1993; 5:864–868. [PubMed: 7694604]
29. Alam N, Goel HL, Zarif MJ, Butterfield JE, Perkins HM, Sansoucy BG, et al. The integrin-growth factor receptor duet. J Cell Physiol. 2007; 213:649–653. [PubMed: 17886260]
30. Ross DT, Scherf U, Eisen MB, Perou CM, Rees C, Spellman P, et al. Systematic variation in gene expression patterns in human cancer cell lines [see comments]. Nat Genet. 2000; 24:227–235. [PubMed: 10700174]
31. Ruffolo EF, Koerner FC, Maluf HM. Metaplastic carcinoma of the breast with melanocytic differentiation. Mod Pathol. 1997; 10:592–596. [PubMed: 9195577]
32. Bachmeier BE, Nerlich AG, Mirisola V, Jochum M, Pfeffer U. Lineage infidelity and expression of melanocytic markers in human breast cancer. Int J Oncol. 2008; 33:1011–1015. [PubMed: 18949364]
33. Rae JM, Creighton CJ, Meck JM, Haddad BR, Johnson MD. MDA-MB-435 cells are derived from M14 Melanoma cells--a loss for breast cancer, but a boon for melanoma research. Breast Cancer Res Treat. 2007; 104:13–19. [PubMed: 17004106]
34. Hughes PE, Diaz-Gonzalez F, Leong L, Wu C, McDonald JA, Shattil SJ, et al. Breaking the integrin hinge. A defined structural constraint regulates integrin signaling. J Biol Chem. 1996; 271:6571–6574. [PubMed: 8636068]
35. Gay LJ, Felding-Habermann B. Contribution of platelets to tumour metastasis. Nat Rev Cancer. 2011; 11:123–134. [PubMed: 21258396]
36. Gon Y, Wood MR, Kiosses WB, Jo E, Sanna MG, Chun J, et al. S1P3 receptor-induced reorganization of epithelial tight junctions compromises lung barrier integrity and is potentiated by TNF. Proc Natl Acad Sci U S A. 2005; 102:9270–9275. [PubMed: 15968000]
37. Panetti TS. Differential effects of sphingosine 1-phosphate and lysophosphatidic acid on endothelial cells. Biochim Biophys Acta. 2002; 1582:190–196. [PubMed: 12069828]
38. Sheu JR, Fong TH, Liu CM, Shen MY, Chen TL, Chang Y, et al. Expression of matrix metalloproteinase-9 in human platelets: regulation of platelet activation in in vitro and in vivo studies. Br J Pharmacol. 2004; 143:193–201. [PubMed: 15289295]
39. Radjabi AR, Sawada K, Jagadeeswaran S, Eichbichler A, Kenny HA, Montag A, et al. Thrombin induces tumor invasion through the induction and association of matrix metalloproteinase-9 and beta1-integrin on the cell surface. J Biol Chem. 2008; 283:2822–2834. [PubMed: 18048360]
40. van Gils JM, Costa Martins PA, Mol A, Hordijk PL, Zwaginga JJ. Transendothelial migration drives dissociation of plateletmonocyte complexes. Thromb Haemost. 2008; 100:271–279. [PubMed: 18690347]
41. Bradfield PF, Scheiermann C, Nourshargh S, Ody C, Luscinskas FW, Rainger GE, et al. JAM-C regulates unidirectional monocyte transendothelial migration in inflammation. Blood. 2007; 110:2545–2555. [PubMed: 17625065]
42. Chavakis T, Keiper T, Matz-Westphal R, Hersemeyer K, Sachs UJ, Nawroth PP, et al. The junctional adhesion molecule-C promotes neutrophil transendothelial migration in vitro and in vivo. J Biol Chem. 2004; 279:55602–55608. [PubMed: 15485832]
43. Iannacone M, Sitia G, Isogawa M, Marchese P, Castro MG, Lowenstein PR, et al. Platelets mediate cytotoxic T lymphocyte-induced liver damage. Nat Med. 2005; 11:1167–1169. [PubMed: 16258538]
44. Iannacone M, Sitia G, Isogawa M, Whitmire JK, Marchese P, Chisari FV, et al. Platelets prevent IFN-alpha/beta-induced lethal hemorrhage promoting CTL-dependent clearance of lymphocytic choriomeningitis virus. Proc Natl Acad Sci U S A. 2008; 105:629–634. [PubMed: 18184798]

45. Italiano JE Jr, Richardson JL, Patel-Hett S, Battinelli E, Zaslavsky A, Short S, et al. Angiogenesis is regulated by a novel mechanism: pro- and antiangiogenic proteins are organized into separate platelet alpha granules and differentially released. Blood. 2008; 111:1227–1233. [PubMed: 17962514]
46. Kisucka J, Butterfield CE, Duda DG, Eichenberger SC, Saffaripour S, Ware J, et al. Platelets and platelet adhesion support angiogenesis while preventing excessive hemorrhage. Proc Natl Acad Sci U S A. 2006; 103:855–860. [PubMed: 16418262]
47. Labelle M, Begum S, Hynes RO. Direct signaling between platelets and cancer cells induces an epithelial-mesenchymal-like transition and promotes metastasis. Cancer Cell. 2011; 20:576–590. [PubMed: 22094253]
48. Gay LJ, Felding-Habermann B. Platelets alter tumor cell attributes to propel metastasis: programming in transit. Cancer Cell. 2011; 20:553–554. [PubMed: 22094248]
49. Labelle M, Begum S, Hynes RO. Platelets guide the formation of early metastatic niches. Proc Natl Acad Sci U S A. 2014; 111:E3053–E3061. [PubMed: 25024172]
50. Dashevsky O, Varon D, Brill A. Platelet-derived microparticles promote invasiveness of prostate cancer cells via upregulation of MMP-2 production. Int J Cancer. 2009; 124:1773–1777. [PubMed: 19101987]
51. Andrews RK, Arthur JF, Gardiner EE. Neutrophil extracellular traps (NETs) and the role of platelets in infection. Thromb Haemost. 2014; 112:659–665. [PubMed: 25265341]
52. Wang Y, Sun Y, Li D, Zhang L, Wang K, Zuo Y, et al. Platelet P2Y12 is involved in murine pulmonary metastasis. PLoS ONE. 2013; 8:e80780. [PubMed: 24236201]
53. Bambace NM, Levis JE, Holmes CE. The effect of P2Y–mediated platelet activation on the release of VEGF and endostatin from platelets. Platelets. 2010; 21:85–93. [PubMed: 20063989]
54. Gebremeskel S, LeVatte T, Liwski RS, Johnston B, Bezuhly M. The reversible P2Y12 inhibitor ticagrelor inhibits metastasis and improves survival in mouse models of cancer. Int J Cancer. 2015; 136:234–240. [PubMed: 24798403]
55. Dovizio M, Alberti S, Sacco A, Guillem-Llobat P, Schiavone S, Maier TJ, et al. Novel insights into the regulation of cyclooxygenase-2 expression by platelet-cancer cell cross-talk. Biochem Soc Trans. 2015; 43:707–714. [PubMed: 26551717]
56. Labelle M, Begum S, Hynes RO. Platelets guide the formation of early metastatic niches. Proc Natl Acad Sci U S A. 2014; 111:E3053–E3061. [PubMed: 25024172]
57. Amo L, Tamayo-Orbegozo E, Maruri N, Eguizabal C, Zenarruzabeitia O, Rinon M, et al. Involvement of platelet-tumor cell interaction in immune evasion. Potential role of podocalyxin-like protein 1. Front Oncol. 2014; 4:245. eCollection@2014.:245. [PubMed: 25309871]

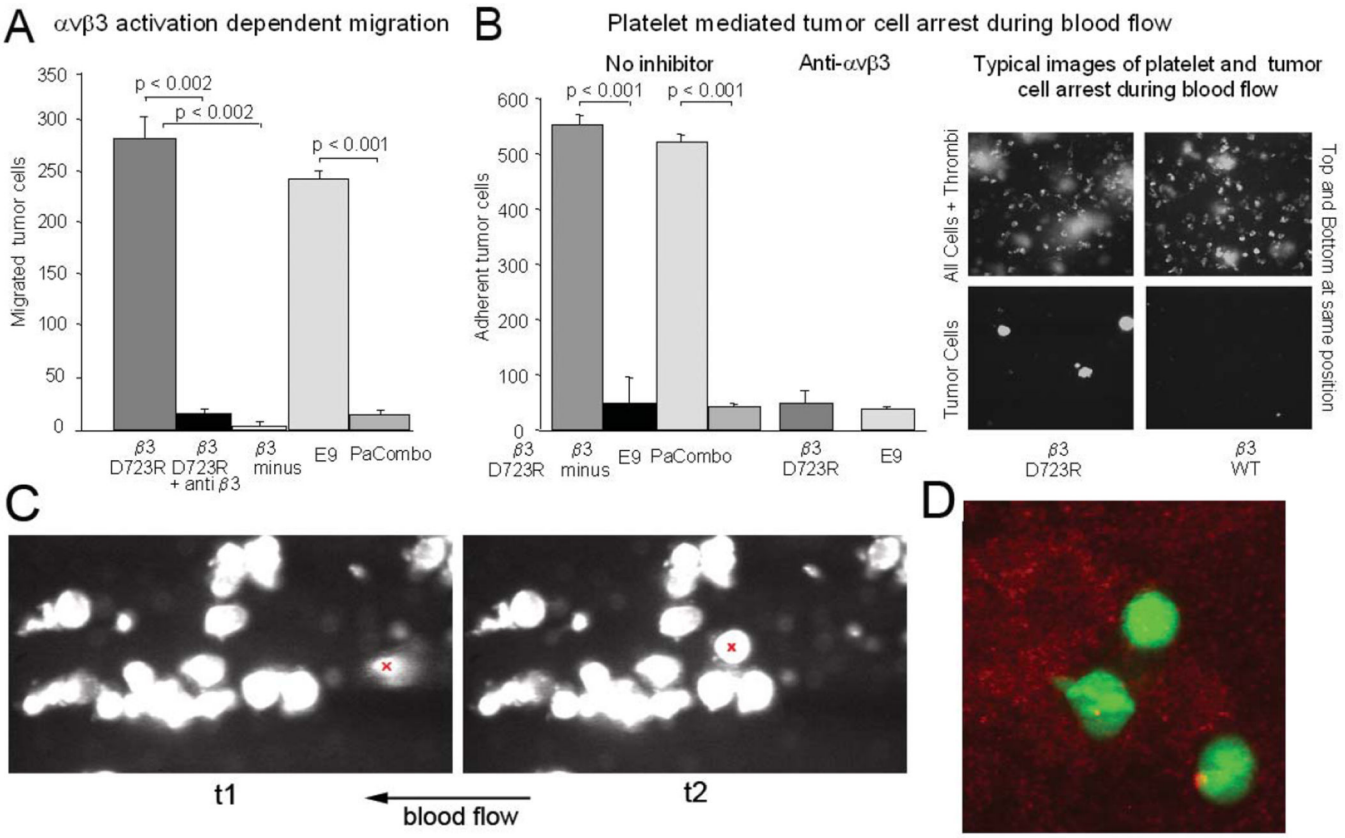

Figure 1. Expression of activated integrin αvβ3 in subpopulations of heterogeneous breast cancer cells and their interaction with platelets during blood flow

A, Haptotactic migration toward immobilized fibrinogen requires activated integrin αvβ3 in MDA-MB 435 cells. Cells selected for lack of β3 expression (β3 minus) failed to migrate in contrast to their counterparts reconstituted with the constitutively activating β3mutant D723R ($p<0.002$). Migration of β3 mutant D723R expressing cells is strongly inhibited by blocking anti-β3 antibody (mab M21-3 at 50 μg/ml) ($p<0.002$). E9, a random clone of MDA-MB 435 cells expresses high affinity αvβ3, while Parent Combo, a combination of 20 MDA-MB-435 clones has low affinity αvβ3 ($p<0.001$) (16 hr migration at 37C). Ooverall expression levels of the integrin are similar across all 435 variants (Fig S1). **B**, Tumor cell attachment to collagen I during blood flow relies on high-affinity integrin αvβ3 (blocked by anti αvβ3 mab VNR1-27.1) and involves platelets. The right panel shows images at predefined positions within a flow chamber, of MDA-MB 435 β3D723R or β3WT expressing cells during blood flow (top images: green fluorescence of arrested leukocytes and platelet aggregates; bottom images: red fluorescence of arrested tumor cells (dsRed) at the same positions). Arrested tumor cells are quantified at 50 predefined positions during ongoing perfusion, after the same number of tumor cells for each cell type were allowed to pass through the chamber. **C**, Dymanic tumor cell-platelet interaction during blood flow. Conditions as in B, but using M21 human melanoma cells in mouse blood. Shown are two consecutive frames of a video microcopy analysis (link to video to be inserted here). The flow field shows a group of tumor cells already attached in a platelet dependent manner. An additional tumor cell, entering the view field, arrests on an existing platelet-tumor

heteroaggregate. This cell is marked with a red ‘x’ in the frames in C, at time points 1 and 2 (t1, t2). Tumor cells can anchor on attached platelets, and sometimes carry platelets at their surface which facilitate tumor cell attachment during blood flow. **D**, Dual-color confocal analysis of tumor cell-platelet interaction during blood flow. M21 melanoma cells (green) interacting with attached, thrombus-forming platelets (red). Upon contact with platelets, tumor cells extend pseudopods (cell in the middle).

Statistical significance in A,B was assessed by paired, one-tailed *t*-tests.

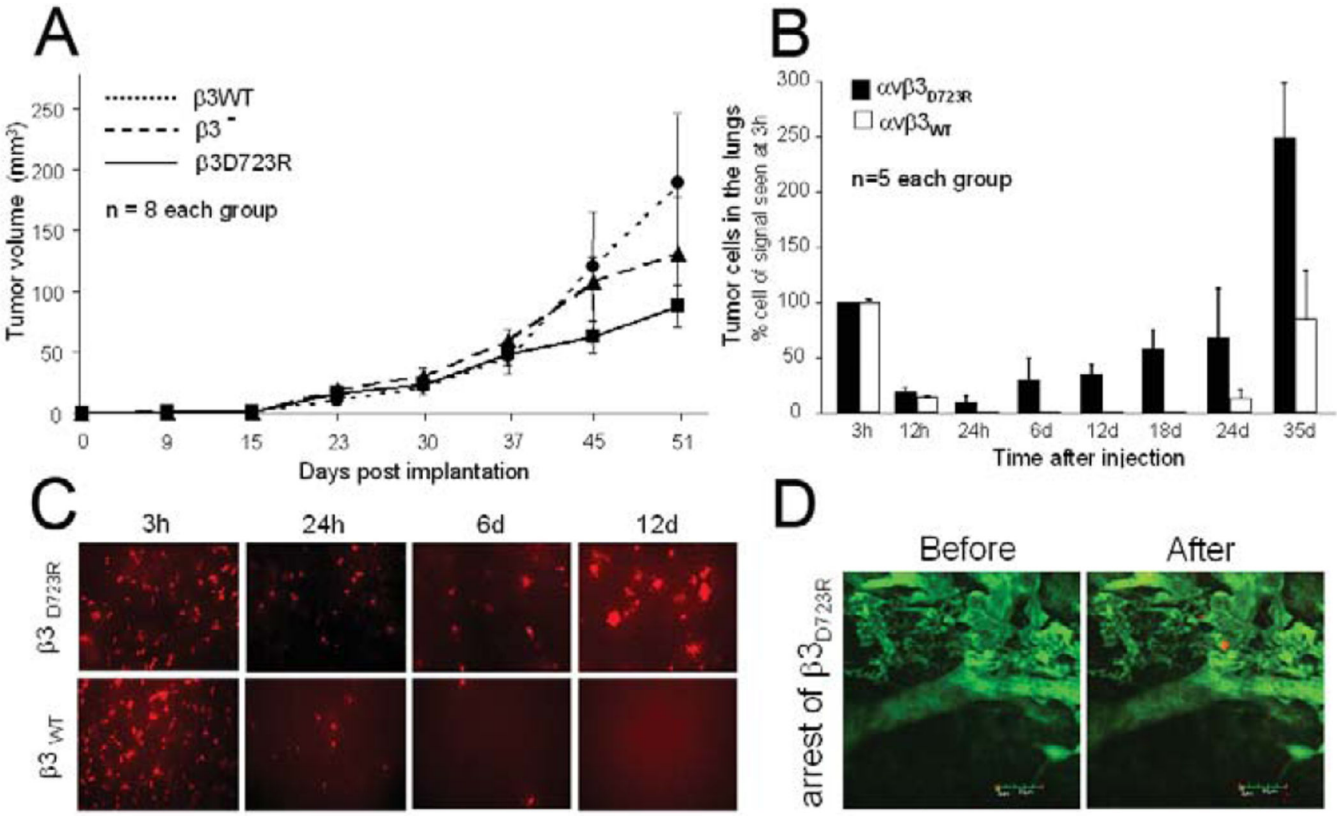

Figure 2. Activation of tumor cell integrin αvβ3 promotes initial steps of target organ colonization from the blood stream but is not required for primary tumor growth

A, Tumor growth in the mammary fat pad of MDA-MB 435 cells lacking β3 expression (β3^{-}), or reconstituted with β3 wild type (β3WT) versus constitutively activating mutant β3 (β3D723R). Tumor volumes in SCID mice (n=8/group) were measured with calipers and calculated as (a^2×b)/2. **B**, Quantification of tumor cells in SCID mouse lungs at varying time points after tail vein injection of 1×10^5 dsRed tagged MDA-MB 435 cells expressing activated αvβ3D723R or non-activated αvβ3WT. Tumor cells were quantified by real time PCR of human *alu* sequences within the lung tissue. Initial signal at 3h post injection was nearly identical for both cell types and reflects tumor cells within the pulmonary microcirculation, most of which are cleared during the first day. Bars indicate numbers of lung associated tumor cells (n=5 mice) shown as % (± SEM) of the initial tumor cell number at 3 hours post injection. Cell numbers are based on PCR standard curves, obtained from lung homogenates spiked with known tumor cell numbers. **C**, Lung whole mounts 3 to 12 hrs after tail vein injection of dsRed tagged tumor cells as in B, visualizing the tumor cells by fluorescence microscopy (10×). Representative fields are shown. **D**, Arrest of β3D723R expressing cells within the pulmonary microvasculature observed by intravital microscopy. Lung allografts were grown in dorsal skin fold chambers on SCID mice, allowed to vascularize for 14 days before superfusion with TNFα (50μl at 1μg/ml) 2.5 hours before i.v. injection of 2.5×10^6 dsRed tagged tumor cells together with FITC-dextran (500 kDa) to visualize the vasculature. Circulation and adhesive events were recorded by intravital video microscopy (Leitz Biomed). Bar, 50 μm.

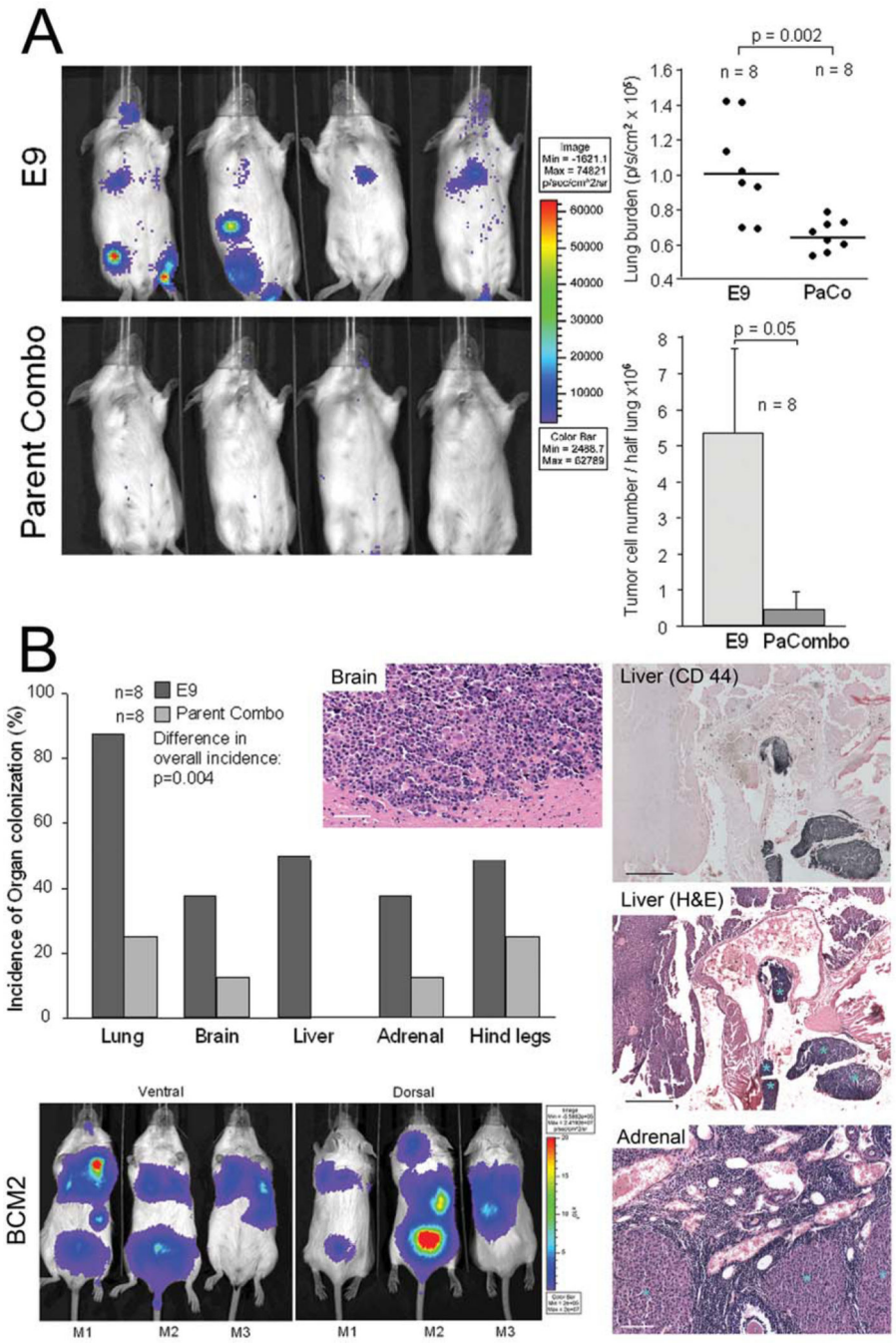

Figure 3. Integrin αvβ3 activation promotes hematogenous metastasis to multiple target organs

A, Left: Metastatic activity of MDA-MB 435 clone E9 expressing intrinsically activated integrin αvβ3 compared to 20-clone pool Parent Combo expressing non-activated αvβ3. Non-invasive bioluminescence imaging of SCID mice 14 days after tail vein injection of 1×10^5 F-luc tagged tumor cells. Right: Quantification of metastatic burden in the lung region by non-invasive bioluminescence imaging, 14 days after injecting 1×10^5 tumor cells (Top), or by real time PCR 34 days after injecting 1×10^6 tumor cells to challenge the system and following the tumor cells by human *alu* sequences (Bottom). Each data point in the top panel

represents signal from one mouse (n=8), the vertical line indicates median signal in each group. Bars in the lower panel show average values (+/− STDEV) for each group (n=8). Clone E9 caused significantly higher metastatic lung burden than clone pool Parent Combo (p=0.002 by bioluminescence imaging 14 days after 1×10^5 injected tumor cells; p= 0.05 by *alu* PCR 34 days after 1×10^6 injected tumor cells). Statistical significance was assessed by paired, one-tailed *t*-tests. **B**, Comparison of target organ colonization by tumor cells expressing activated versus non-activated αvβ3. Incidence of tumor cell burden in the lungs, brain, liver, adrenal glands and bone (hind legs), 56 days after tail vein injection of 1×10^5 clone E9 cells versus clone pool Parent Combo. Organ associated metastatic burden was detected in excised organs by *ex vivo* bioluminescence imaging, n= 8 mice / group. The presence of metastatic lesions was verified by histology (right panels). Brain lesion H&E staining, Bar 80 μm. Liver lesion, top panel identifies tumor lesions by immunohistochemistry with anti human CD44 (Mab 29.7) (dark blue), bottom panel shows a neighboring section stained with H&E and lesions marked with blue asterisks, Bar 200 μm. Adrenal gland section shown by H&E staining, lesions marked with light blue asterisks, Bar 150 μm. Mouse images: Multiple target organ colonization validated with polyclonal cell population BCM2 which express activated integrin αvβ3. Non-invasive bioluminescence imaging of metastasis development in distinct target organs, 56 days after tail vein injection of 2.5×10^5 tumor cells. Three representative mice are shown (ventral and dorsal). Metastatic burden in the lungs, liver, brain, spine, and adrenal gland was confirmed by bioluminescence imaging of the excised organs, and by histology as above.

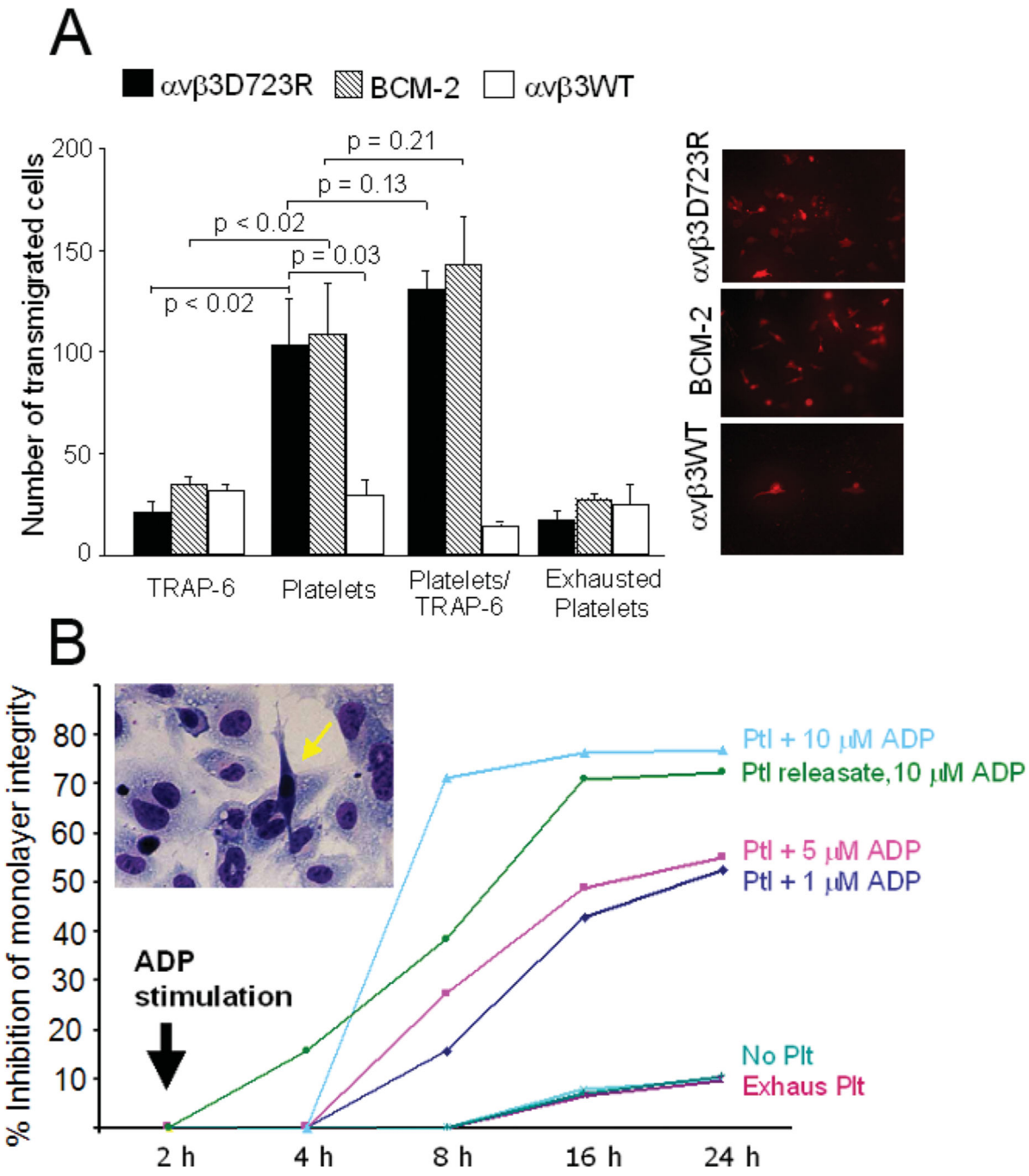

Figure 4. Activated integrin αvβ3 promotes tumor cell transendothelial migration in a platelet dependent manner

A, Platelets and high affinity tumor cell integrin αvβ3 together promote tumor cell transendothelial migration *in vitro*. In the presence of platelets, MDA-MB 435 cell variants expressing high affinity αvβ3D723R, or intrinsically activated αvβ3 (BCM2), penetrated monolayers of human lung microvascular endothelial cells more efficiently than tumor cells with low affinity αvβ3WT (p=0.03). Platelet activation with TRAP-6 (thrombin receptor activating peptide-6 and PAR1 agonist) before incubation with tumor cells did not further

enhance the stimulatory effect. TRAP-6 alone without platelets, or exhausted platelets (stimulated with TRAP-6, allowed to release their α granules, and washed before addition to tumor cells), did not enhance tumor cell transendothelial migration. **B**, Platelet releaseate reduces endothelial monolayer integrity in the presence of tumor cells. Intact human pulmonary endothelial layers (initial transendothelial resistance >30Ω/cm^2) were incubated with BCM2 cells, and washed human platelets stimulated with ADP, or their ATP induced releasates were added. Transendothelial resistance was measured at the indicated time points. Insert shows damaged endothelial layer with a tumor cell crossing over into a denuded area (yellow arrow).

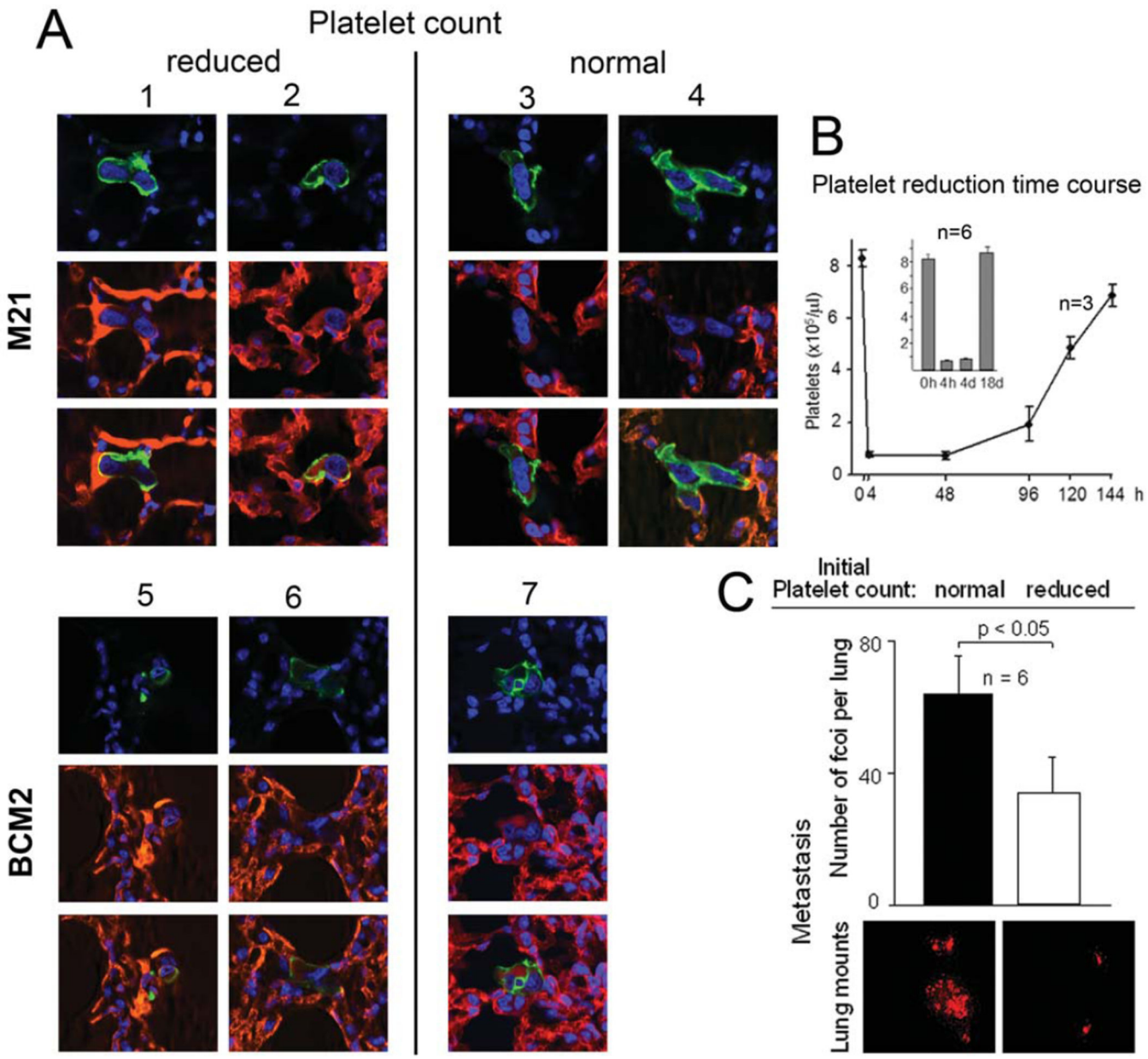

Figure 5. Platelets promote tumor cell extravasation and metastasis from the blood stream *in vivo*

A, Tumor cell extravasation from the pulmonary microvasculature in SCID mice with reduced or normal platelet counts. Thrombocytopenia was induced with anti-murine platelet GP1bα 4 hrs before i.v. injection of M21 melanoma or BMC2 breast cancer cells. Extravasation was analyzed by confocal microscopy on day 3, revealing tumor cells (human CD44 in green) inside the vasculature (CD31, PECAM in red) in thrombocytopenic mice (mouse# 1,2,5,6), or outside the vasculature in mice with normal platelet counts (mouse# 3,4,7). **B**, Platelet reduction time course. Thrombocytopenia was induced as in A (n=3), and platelet counts measured at the indicated time points. Insert shows platelet counts in mice in which experimental metastasis, measured in C (n=6). **C**, Thrombocytopenia reduces

metastasis from the blood stream. SCID mice were injected with anti platelet glycoprotein GPIbα as above, or PBS as control (n=6). Four hours later, 1×10^5 sdRed tagged BCM2 tumor cells were injected into the tail vein and lung metastases counted microscopically in whole mounts of each lung lobe, 18 days later. Bars denote the number of metastatic foci per lung ± SEM, counted regardless of size. Images below show dsRed tumor cell lesions in lung whole mounts representative for each experimental group. Mice with normal platelet counts had significantly more metastases ($p<0.05$) than thrombocytopenic mice. Generally, lesions in control mice were also considerably larger than lesions in anti-platelet treated mice. Differences in metastatic burden were confirmed by real time PCR of human *alu* sequences within the lung tissue (not shown). Statistical significance was assessed by paired, one-tailed *t*-tests.

Table 1

Effect of platelets on tumor cell extravasation and early metastasis in vivo

Morphometric measurements of mouse lung sections 3 days after i.v. injection of MDA-MB-435 β3D723R or BCM2 cells. Each cell type was injected into mice with normal or 10-fold reduced platelet counts (n=2/condition). Data for each mouse indicate the analyzed lung area, numbers of metastases found (lesion count regardless of size), number of metastases/area, percentage of lesions found intravascular (intact vascular endothelium/basement membrane), or near blood vessels with broken vascular basement membrane and endothelium indicating extravasation. Also included is the percentage of lesions showing BrdU uptake (24 h *in vivo* pulse) indicating proliferative activity, regardless of lesion size. Tumor cell lesions in mice with normal platelet counts were generally considerably larger and had higher proliferative activity than lesions in thrombocytopenic mice. Localization of intravascular and extravascular tumor cells was confirmed by confocal microscopy as shown in Fig. 5A.

Tumor cell type	Platelet count	Measured lung area (mm^2)	Number of metastases in measured area	Number of metastases / mm^2	% extravasated	% BrdU positive
α3D723R	normal	85.3 140.2	35 83	0.410 0.592	100 95	68.6 62.4
α3D723R	reduced	109.6 126.2	9 22	0.082 0.174	0 0	15.5 18.6
BCM2	normal	84.4 88.7	52 38	0.616 0.428	92 100	67.2 63.0
BCM2	reduced	84.3 86.7	14 18	0.166 0.207	7 0	12.2 14.4